Mining Science, vol. 32, 2025, 241-252

www.miningscience.pwr.edu.pl

Mining Science

(Previously Prace Naukowe Instytutu Gornictwa Politechniki Wroclawskiej, ISSN 0370-0798)

ISSN 2300-9586 (print)
ISSN 2353-5423 (online)

Received October 7, 2025; Reviewed; Accepted December 31, 2025

EXAMINING THE EFFECT OF PRECIPITATION ON ERT MONITORING MEASUREMENTS BY STATISTICAL APPROACH

Marcell KÁRPI[1]*, Krisztián Mátyás BARACZA[2], Sándor SZALAI[3]

[1,2] Research Institute of Applied Earth Sciences, University of Miskolc, Hungary
[3] Institute of Earth Physics and Space Science (ELKH-EPSS), Sopron, Hungary

Abstract: The study examines the impact of precipitation on the distribution of apparent specific electrical resistivity (ρ_a) in the soil through statistical analysis of data measured in a direct current geoelectric Dipole-Dipole (DPDP) electrode array in the park of the University of Miskolc, on an artificially constructed area. Following data filtering, regression analysis (Montgomery et al., 2012) and analysis of variance (ANOVA) (Montgomery, 2012; Kim, 2014) were applied to investigate the relationship between precipitation and ρ_a. Separate analyses were conducted for each measured depth level as a function of the precipitation amount recorded over the three months prior to the geoelectric measurements. The combined application of statistical methods provides an effective tool for understanding the hydrogeological state of the soil and the dynamics of subsurface water movement, while considering the influence of environmental factors and human activity. The results of the study may be valuable for interpreting data provided by monitoring systems and for shallow geophysical investigations aimed at mapping the hydrogeological functioning of an area.

Keywords: *regression analysis, ANOVA, ERT, monitoring, precipitation*

1. INTRODUCTION

In geophysical engineering the first decision is always finding the best appliable, and most economical method to the given problem. These methods rely on different physical phenomena that have their own limitations. The uncertainties discussed in this study is the direct current geoelectrical monitoring method, or ERT as commonly referenced. Since the method works with current injected to the subsurface, precipitation is

* Corresponding author: marcell.karpi@uni-miskolc.hu (M. Kárpi)
doi: 10.37190/msc/217537

a key question that needs to be examined. The study aims to approach a rather unprecedented methodology: applying statistical evaluation to raw measured monitoring data, from repeated measurements through a four years window. Statistical processing and interpretation of geoelectric data are advantageous in shallow geophysical investigations, as they enable a more complex yet reliable examination of subsurface structures. One of the most critical practices following measurements is the identification and handling of erroneous or outlier data, which may arise from noisy environments or measurement errors. Filtering such data is essential, as they can significantly distort inverted images (Isaaks et al., 1989). Although there are inversion solutions, such as those using the L1 norm (the sum of the absolute values of a vector's components), which is less sensitive to outliers, the study only works with ρ_a datasets, therefore manual data filtering had to be applied to the geoelectric data to eliminate unrealistically high values clearly resulting from measurement errors. The measurements were conducted in the park of the University of Miskolc under varying precipitation conditions and with monitored meteorological histories. Polynomial regression analysis (Montgomery et al., 2012) was performed to explore potential relationships between precipitation and ρ_a. The measurements aimed to observe the effect of precipitation on the geoelectric resistivity of the soil, considering the geological characteristics of the profile. The investigated area was dominated by valley-foot debris prior to filling, upon which construction debris was deposited in multiple layers of varying thickness decades ago, followed by a cover of locally available clayey soil several tens of centimetres thick. These layers, mixed with significant clay content, behave as good electrical conductors. As expected, specific resistivity decreases under wet conditions, while an increase in resistivity is observed during dry periods. At the outset of the measurements, a key question was to determine the depth to which geoelectric monitoring could detect the effects of wet and dry periods in the given area. This behaviour is closely related to the soil's properties, such as its water-holding capacity and the presence of dissociated ions in the pore space. Different soils and rocks respond uniquely to various weather conditions (Cheban et al., 2014). The selected study area at the University of Miskolc represents a transition between low- and high-permeability soils. The results indicate a slight negative correlation between precipitation and ρ_a. The low slope of the polynomial regression models suggests that increased precipitation causes only minor changes in the ρ_a values of the middle and deeper soil layers, consistent with the soil's clay content and the conductivity of near-surface layers. By exploring the relationships between changes in the water balance and electrical conductivity, more accurate conclusions can be drawn about the area's moisture content and the dynamics of subsurface water movement. It is important to note that geoelectric measurement results are influenced not only by precipitation but also by other environmental factors, such as temperature, vegetation, or the degree of anthropogenic disturbance. The findings of this study also highlight the extent to which changes in environmental parameters can affect measured resistivity values. This is particularly significant for the design of monitoring systems aimed at accurately tracking

long-term changes. The research focused on analysing measured DPDP data and precipitation conditions using two-way ANOVA and polynomial regression. The study exclusively utilized ρ_a data, and inversion results are not discussed in this manuscript. Based on the findings, the combined use of statistical analyses suggests a simple yet potentially effective tool for monitoring the hydrodynamic state of the soil, which may prove useful in future shallow geophysical investigations.

1.1. LITERATURE REVIEW

Long-term multielectrode geoelectric monitoring with fixed electrical resistivity tomography (ERT) arrays has proven highly effective for quantifying the influence of precipitation on subsurface apparent resistivity and soil moisture over extended periods, revealing both rapid event-scale responses and gradual multi-annual trends (Whiteley et al., 2019; Hojat et al., 2022). In Vertisols, for example, seasonal wetting–drying cycles driven by cumulative rainfall produce resistivity variations exceeding one order of magnitude (10–500 Ωm to <50 Ωm), with the most dramatic decreases occurring during the first major rainfalls after prolonged dry periods when desiccation cracks facilitate rapid infiltration (Amidu and Dunbar, 2007). Permanent ERT installations on landslide-prone slopes consistently record sharp resistivity reductions of 30–70 % in the upper 5–15 m within 12–72 hours of intense precipitation (>20–50 mm/day), often followed by partial recovery over weeks as drainage occurs; these transient low-resistivity zones directly precede measurable displacement in many cases, underlining the value of geoelectric monitoring for early-warning systems (Supper et al., 2014; Palis et al., 2017; Uhlemann et al., 2017). Depth-dependent behaviour is a recurrent observation: near-surface pseudosections (0–3 m) typically show high-amplitude, short-term fluctuations tightly coupled to individual rainfall events, whereas deeper levels (8–20 m) exhibit damped, lagged responses or even inverse trends controlled by capillary rise, matrix flow, or redistribution through permeable layers (Carrière et al., 2013; Zhao et al., 2020; Scaini et al., 2021). In a loess landslide, Zhao et al. (2020) documented downward migration rates of low-resistivity fronts of approximately 0.3–0.8 m/day following heavy rain, while Watlet et al. (2018) tracked focused infiltration along karst conduits that remained active for up to 40 days after rainfall ceased, generating localised resistivity anomalies <10 Ωm that propagated from the surface to cave systems at depths of 30–50 m. Agricultural and hillslope studies further illustrate the dominance of cumulative annual precipitation on bulk resistivity, with sites receiving >800 mm/year showing sustained low-resistivity periods throughout the wet season, whereas calcic horizons or clay-enriched layers act as effective barriers that restrict deep percolation and maintain elevated moisture (and thus lower resistivity) in the overlying vadose zone for months (Kotta et al., 2020; Scaini et al., 2021). Time-lapse inversion results frequently report seasonal true-resistivity contrasts of 200–300 % between dry and wet states, yet most published works rely on visual comparison of inverted tomograms, percentage-change

maps, or simple linear correlation with rainfall totals rather than formal statistical modelling of the apparent resistivity time series itself (Brunet et al., 2010; Hojat et al., 2022). Quantitative petrophysical conversion using Archie's or Waxman-Smits models is occasionally applied, but calibration is challenging in heterogeneous soils and often limited to point-scale neutron probe or TDR validation (Scaini et al., 2021). Consequently, while inversion-based 4D-ERT provides spatially distributed images of moisture evolution, the direct statistical treatment of long-term apparent resistivity data—particularly when stratified by investigation depth—remains relatively scarce.

The approach of applying polynomial regression and variance analysis directly to multi-year sequences of apparent resistivity values extracted at discrete depth levels offers a robust, inversion-independent framework that explicitly quantifies the magnitude, nonlinearity, and statistical significance of precipitation effects across the subsurface profile. Compared to the predominantly qualitative or inversion-centred methodologies that dominate the literature (e.g., Supper et al., 2014; Uhlemann et al., 2017; Whiteley et al., 2019), this statistically driven analysis of raw apparent resistivity data provides a lightweight yet rigorous complement capable of detecting subtle depth-specific trends and threshold behaviours that may be obscured by inversion artefacts or smoothing constraints, thereby enhancing the interpretive power of permanent geoelectric monitoring arrays for hydrological and geotechnical applications.

2. MATERIALS AND METHODS

2.1. THE ERT METHOD

Geoelectric methods are the second most widely used geophysical techniques after seismic methods, applied extensively in solving hydrogeological, environmental, engineering geological, and archaeological problems. Their popularity stems from their broad applicability. Direct current geoelectric methods are primarily used for shallow investigations (penetrating a few hundred meters). Their operating principle involves injecting current into the ground through electrodes A and B, while measuring the potential difference between measuring electrodes M and N. In specific cases, three- or two-electrode configurations or focusing arrangements are also employed. The measured data, ρa reflects the average properties of the rock surrounding the electrode arrangement. In this study, the DPDP electrode configuration was used due to its excellent horizontal sensitivity. Nowadays, measurements are often conducted using multielectrode systems (Figure 1.), where a computer controls the operation of current and potential electrodes.

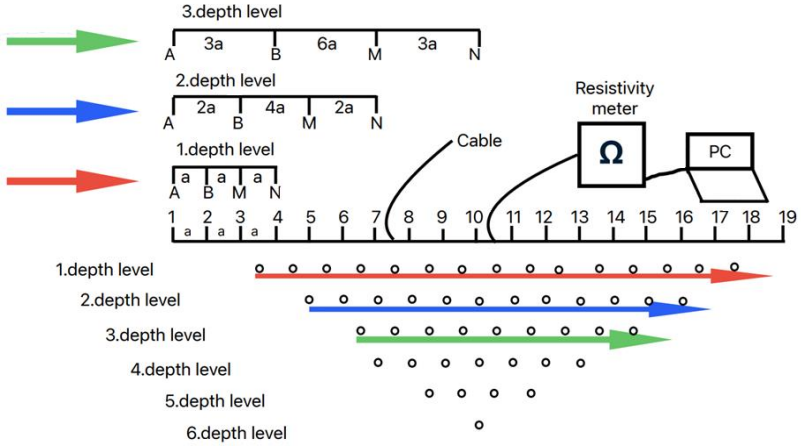

Fig. 1. Illustration of direct current multielectrode ERT measurement with DPDP array (Szalai, 2020)

During two-dimensional (2D) measurements, electrodes are placed in a line at fixed intervals, enabling simultaneous investigation of vertical and horizontal variations in specific resistivity. The measured data can be converted into true specific resistivity using inversion techniques, achieved by iteratively refining an initial model to minimize the discrepancy between measured and calculated data. Due to the indirect nature of geoelectric data, the profile must be interpreted in the context of geological conditions.

2.2. THE STUDY AREA PARAMETERS

In Table 1 the lithological and geoelectric parameters can be seen of the study area. The campus of the University of Miskolc was a marshland in the past, before the government built the university, the area was drained and filled up with construction debris. The thickness and composition of this compacted debris changes everywhere, but the layers were examined in a waterpipe trench near to the geoelectric sections, giving reliable information for the measurement. Though the permeability and porosity varies greatly in this layer, it is expected that precipitation induced geoelectrical response change is measurable to at least a certain depth. The undermost layer serves as a water basin in the valley, collecting the waters from the sides, with very low permeability.

Table 1. Calculated parameters in representative depths

Lithology	Depth [m]	Porosity [%]	Permeability [mD]	ρa [Ω]
Clayey soil	0-0.25	25	100	5-15
Compacted construction debris (inhomogenous)	0.25-3	15-40	10-100	200
Weathered andesite tuff /compact clayey soil	3-	2-8	0.1	500

2.3. THE APPLIED STATISTICAL METHODS

The application of statistical methods in processing geophysical data is highly effective for uncovering the structure, relationships, and reliability of measured data. In the analysis of geoelectric measurements, detailed statistical evaluation enables the exploration of temporal changes in the electrical properties of the soil and the quantification of the impact of precipitation conditions. In this study, descriptive statistical measures were used to determine the fundamental characteristics of the dataset. These include the correlation analysis, regression analysis, and variance analysis. Interquartile range (IQR) was used to quantify the distribution characteristics of the variables. These measures provide a statistical summary of the data and facilitate the identification of potential anomalies or outliers. Correlation analysis examines the strength and direction of relationships between different measurement parameters. Regression analysis enables the prediction of a dependent variable (e.g., ρ_a) based on one or more independent parameters (e.g., precipitation amount). In addition to linear regression, the method can be extended to multivariate models to uncover more complex relationships. The parameters of the regression model, such as the slope (beta) and the goodness of fit (R^2), provide a more precise understanding of these relationships. Analysis of variance (ANOVA) is used to investigate significant differences between the means of multiple groups. This method is particularly useful for comparing measurements taken at different time points, such as evaluating differences in specific resistivity values measured across different years, while still considering the precipitation. Based on the F-statistic and its associated p-value, it can be determined whether the differences are statistically significant or the result of random fluctuations. The statistical analyses performed provide a robust foundation for interpreting the measured data. These geostatistical tools enabled a detailed analysis of the impact of precipitation, the identification of anomalies, and the evaluation of the significance of differences in specific resistivity values measured across different periods. The results contribute to a better understanding of subsurface processes and the further development of monitoring systems in the field of shallow geophysical investigations.

2.4. DATA FILTERING

During the data filtering process, the ρ_a values of the geoelectric DPDP data were examined, and erroneous or outlier values were filtered out from the dataset. The initial step involved a visual inspection of the data using boxplot visualization. The boxplot enabled rapid identification of the data distribution and any extreme values. In the next step, outliers were filtered using the IQR based on quartiles. The lower boundary is calculated by Q1-1.5xIQR, while the upper boundary is given by Q3+1.5xIQR. Additionally, manual constraints were applied to the ρ_a values to prevent unrealistically high values from distorting the analyses. The upper limit was set at 5000 Ωm, and the lower

limit at -5000 Ωm, because from experience it is known, that these values are the realistic measured limits with the method, values exceeding these limits are usually measurement errors. Identified outliers were replaced using linear interpolation. The quality of the measurement was good, with less than 3% of the points removed and reinterpolated. During interpolation, values were recalculated based on neighbouring data points, ensuring the continuity of the dataset while preventing extreme values from further distorting the analysis. The proportion of outliers was quantified and examined using a representativeness factor, expressed as a percentage, but not displayed in this study. Given the test area has a rather simple layer structure, and free of unknown anomalies, there was no risk of removing the outliers. The complete data cleaning process improved the reliability of the dataset by removing erroneous values, thereby minimizing their distorting effects. The executed data cleaning process provided a stable foundation for the statistical analyses conducted in subsequent stages.

3. RESULTS

3.1. REGRESSION ANALYSIS OF PRECIPITATION ON ARS

To investigate the joint changing of ρ_a and precipitation, several curve fitting methods were tried, and finally second degree polynomial regression analyses was chosen to be showcased. Figure 2. illustrates the relationship between precipitation amount (mm) and ρ_a at the representative depth of 25 cm. Due to constraints, we only subject to display the depth level, in which the correlation is the strongest. In the analysis, second-degree polynomial regression fit (calculated curve) was applied to describe the nonlinear changes occurring with increasing precipitation. The results in Figure 2. reveals a nonlinear inverse relationship between ρ_a and precipitation, averaged over the preceding four months, with data points clustered by measurement dates from 2019 to 2024. The fitted curve exhibits a hyperbolic decay, where higher precipitation levels correspond to markedly lower apparent resistivity values, approaching asymptotic behaviour near $\rho_a \approx 10–20$ Ωm for precipitation exceeding 30 mm, while drier conditions (precipitation < 10 mm) yield elevated resistivity up to 50 Ωm. This pattern indicates soil moisture saturation effects in the near-surface layer. In the context of the site's hydrogeological setting -an artificially infilled marshland comprising construction debris and clay-rich soils within a drainage basin- the observed resistivity reduction with increased precipitation reflects enhanced electrolytic conduction due to pore water infiltration, albeit moderated by the low permeability of clay matrices that promote surface runoff and lateral drainage via engineered channels to an adjacent river. The quadratic curvature suggests a threshold-driven response: initial precipitation increments rapidly decrease resistivity through partial wetting of heterogeneous fill materials, but further inputs lead to diminished marginal effects as the soil approaches hydraulic saturation, with persistent groundwater presence facilitating capillary rise and maintaining baseline conductivity even during

low-precipitation periods; this implies seasonal recharge dynamics where episodic heavy rains in wetter years (e.g., 2020–2021) overwhelm drainage capacity, potentially exacerbating localized waterlogging in the debris-laden subsurface, while prolonged dry spells in 2024 elevate resistivity through desiccation cracking in clays, thereby influencing aquifer vulnerability to contamination transport along preferential flow paths.

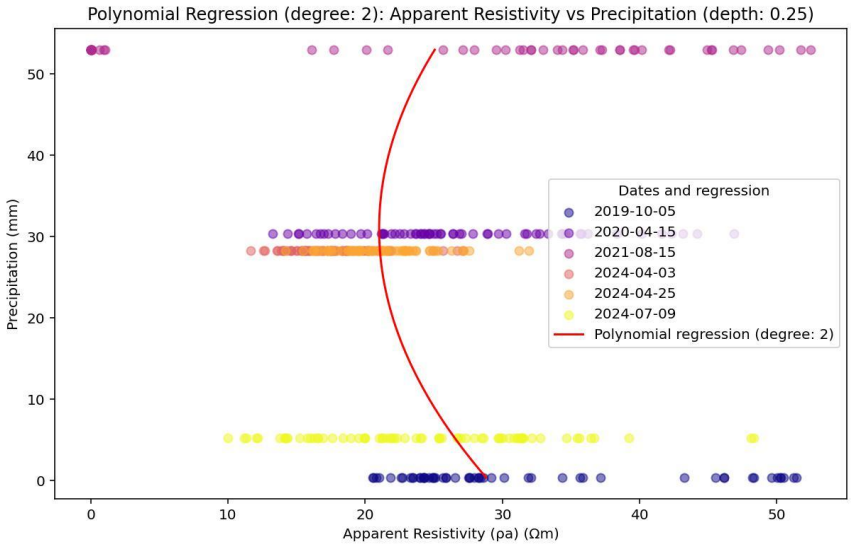

Fig. 2. Polynomial regression graph of the DPDP data, 25cm penetration depth

3.2. CORRELATION ANALYSIS

Across the entire depth range, it can generally be concluded that the average correlation is weakly negative, with its minimum at 3.75 m depth (strongest negative relationship) and maximum at 6.5 m (strongest positive relationship). Based on R^2, the model fit is weak, with the best fit occurring at 7.25 m depth. The average MSE is 27.87, with the highest error at 0.375 m depth. The correlation exhibits a slightly positive relationship with depth (correlation: 0.28). This indicates that in shallow layers (0-4 m), negative correlation is more prevalent (increased precipitation reduces resistivity, e.g., due to soil moisture), but it weakens with depth and occasionally becomes positive. The most negative range is around 3-4 m (-0.17 to -0.20). A weak negative relationship exists with depth (-0.18). The fit is generally weak ($R^2 \approx 0$ or negative), but improves at some deeper points (e.g., 7.25m: 0.44; 7.5m: 0.37). This suggests that the polynomial model may better capture nonlinear relationships in deeper layers. A strong negative relationship (-0.73) is observed. The error decreases drastically with increasing depth: high in shallow layers (e.g., 0-1m: ≈76), low in deeper ones (e.g., 5-6 m: ≈4-5). This

may indicate greater variability in shallow layers (e.g., due to meteorological effects), whereas values are more stable at greater depths. Table 2 lists the main calculated parameters of correlation and error of model, in the three main depth domains, two levels for each domain.

Table 2. Calculated parameters in representative depths

Depth (m)	Correlation	R^2	MSE
0.25	-0.13	0.08	83.36
0.5	-0.08	0.21	82.26
3.0	0.08	-0.02	37.87
4.0	-0.16	-0.00	22.89
5.125	-0.00	0.01	5.12
6.875	-0.06	-0.16	8.02

3.3. PHYSICAL ASSUMPTIONS

Based on site-specific insights, the clay-dominated soil exhibits strong electrical conductivity due to abundant free ions on particle surfaces, with resistivity further declining in moist conditions as pore water enhances electrolytic pathways. Dry periods induce only modest resistivity increases while maintaining overall low values, aligning with the expected gentle negative regression slope in shallow subsurface zones. Stratigraphic anomalies temper correlations between extreme precipitation and apparent resistivity shifts, as the thalweg positioning within a vast catchment ensures residual moisture retention that averts detectable drying effects. Spatial variability in precipitation, coupled with heterogeneous compaction and porosity from the former marsh's infilling with debris, further dilutes direct hydrogeological responses, underscoring the role of subsurface heterogeneity in modulating infiltration and recharge patterns.

3.4. ANOVA (VARIANCE ANALYSIS)

The temporal variability of ρ_a considering the precipitation, was assessed at each depth level using two-way ANOVA, an extension of one-way ANOVA that simultaneously evaluates the effects of two categorical predictors -here, measurement date (Datum) and precipitation level (P_level)- along with their interaction on a continuous response variable (ρ_a). The model specification was Rho ~ C(Datum) x C(P_level), where P_level was derived globally by tercile binning of the four-month mean precipitation that included the survey month and the three preceding months. Computations were performed separately for each depth level using ordinary least-squares regression followed by Type-II ANOVA in the statsmodels framework.

At 0.25m depth (Fig. 3), the analysis revealed one of the strongest overall effects ($F(5,\infty) = 54.60$; $p < 10^{-5}$). The 2019-10-05 campaign yielded a stable ρ_a median near 30 Ωm with a broad interquartile range (IQR), reflecting considerable lateral heterogeneity despite belonging to the "Low precipitation" category. The 2020-04-15 survey (Medium) exhibited a reduced median of ~25 Ωm and an IQR compressed to one-third of the previous width, indicating spring precipitation-induced homogenization. The 2021-08-15 record (High) collapsed to a single outlier, consistent with pore-space saturation during extreme summer rainfall. The 2024 campaigns (Low) reverted to elevated medians (28–32 Ωm) and narrow IQRs, underscoring soil moisture memory: the thalweg position of the site sustains sufficient saturation to buffer ρ_a even under nominally dry conditions.

The interaction term (Datum × P_level) proved highly significant ($p < 10^{-9}$), suggest that precipitation influence is seasonally modulated rather than additive. During wet periods, lateral ρ_a scatter diminishes dramatically; during dry periods, antecedent saturation limits the expected resistivity rise. This pattern is most pronounced at 0.25 m and explains the absence of a detectable global P_level main effect: the influence is strictly context-dependent and emerges only through the interaction term.

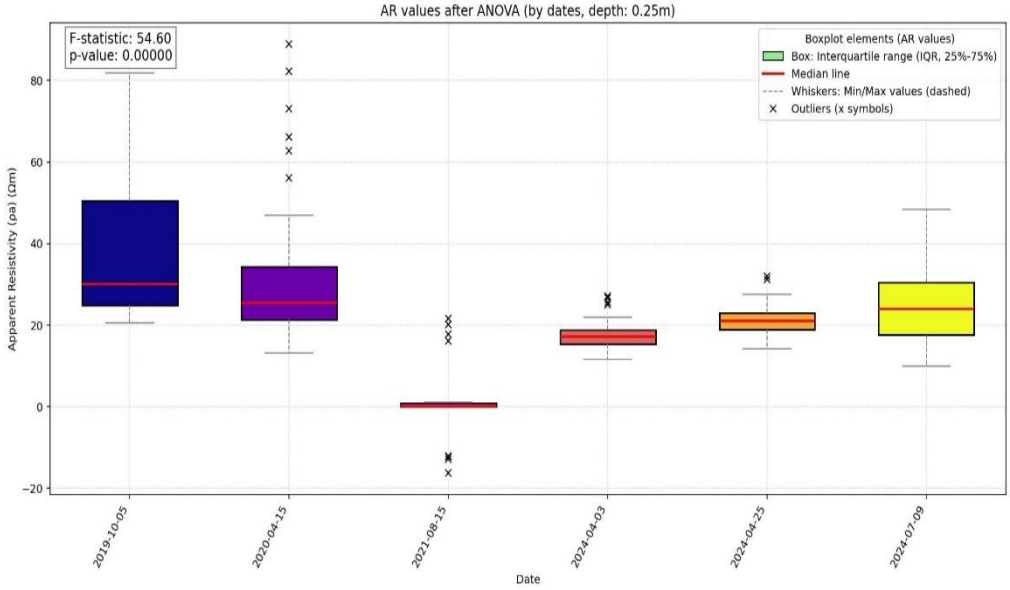

Fig. 3. Results in the first depth level (25cm), where the variance is the most significant

4. CONCLUSION

The results conclusively suggest that the linkage between geoelectric monitoring and antecedent rainfall is far from univocal. Far more intricate interplays governed by

lithology, rock-physical parameters, and pore-scale heterogeneities ultimately dictate measured ρ_a. Regression analysis reveals a negative covariance in the vadose zone that systematically attenuates with depth, mirroring the progressive hydraulic damping of meteoric recharge. ANOVA indicates statistically resolvable shifts in ρ_a populations down to intermediate depths; however, these shifts cannot be ascribed univocally to rainfall totals in every horizon. By fusing regression and ANOVA, we gain a framework with potentialfor anomaly detection, data-quality assurance, and the disentangling of spatial versus temporal controls. This dual-statistical workflow elevates the fidelity of DC geoelectric datasets and highlights threshold-driven hydrogeophysical responses. The statistically evaluateddataset from the University of Miskolc campus gives an insight to the physical processes of areas with similar geology, therefore can constitute a good base for future research.

ACKNOWLEDGEMENTS

The research was carried out in the framework of the GINOP-2.3.2-15-2016- 00010 "Development of enhanced engineering methods with the aim at utilization of subterranean energy resources" project of the Research Institute of Applied Earth Sciences of the University of Miskolc in the framework of the Széchenyi 2020 Plan, funded by the European Union, co-financed by the European Structural and Investment Funds.

REFERENCES

Amidu SA, Dunbar JA. 2007. Geoelectric studies of seasonal wetting and drying of a Texas Vertisol. *Vadose Zone Journal 6: 511-523.*

Brunet P, Clément R, Bouvier C. 2010. Monitoring soil water content and deficit using Electrical Resistivity Tomography (ERT): A review of recent progress. *Journal of Hydrology 393: 158-170.*

Carrière SD, Chalikakis K, Danquigny C, Davi H, Mazzilli N. 2013. Influence of rainfall on the infiltration process in a karst system: A case study in the Cévennes area (France). *Hydrogeology Journal 21: 1807-1822.*

Cheban A, Huraj V, Marcin M. 2014. Modeling of groundwater recharge using a multiple linear regression (MLR) recharge model developed from geophysical parameters: a case of groundwater resources management. *Journal of Hydrology and Hydromechanics 62: 227-235.*

Hojat A, Arosio D, Ivanov VI, Longoni L, Papini M, Scaioni M, Tresoldi G, Zanzi L. 2022. Time-Lapse Electrical Resistivity Tomography (TL-ERT) for Landslide Monitoring: Recent Advances and Future Directions. *Applied Sciences 12: 1425.*

Isaaks EH, Srivastava RM. 1989. An Introduction to Applied Geostatistics. Oxford University Press.

Kim HY. 2014. Analysis of variance (ANOVA) comparing means of more than two groups. *Restorative Dentistry & Endodontics 39: 74-77.*

Kotta D, Kutta K, Godio A. 2020. Monitoring Soil Moisture Dynamics Using Electrical Resistivity Tomography under Homogeneous Field Conditions. *Sensors 20: 5505.*

Montgomery DC. 2012. Design and Analysis of Experiments. *8th ed. John Wiley & Sons.*

Montgomery DC, Peck EA, Vining GG. 2012. Introduction to Linear Regression Analysis. *5th ed. John Wiley & Sons.*

Palis E, Lebourg T, Trigo L, Vidal M, Fabre S. 2017. Long-term monitoring of a large deep-seated landslide using time-lapse electrical resistivity tomography. *Engineering Geology 221: 1-12.*

Scaini A, Sánchez N, Vicente-Serrano SM, Martínez-Fernández J. 2021. Soil structure and soil moisture dynamics inferred from time-lapse electrical resistivity tomography. *Catena 203: 105342.*

Supper R, Baron I, Ottowitz D, Motschka K, Gruber S, Winkler E, Jochum B. 2014. Geoelectrical monitoring: An innovative method to supplement landslide surveillance and early warning. *Landslides 11: 815-830.*

Szalai S. 2020. Examination of geoelectric quasi-null arrays, and small-scale crack systems. *MTA Doctoral Dissertation.*

Uhlemann S, Chambers J, Wilkinson P, Maurer H, Merritt A, Gunn D, Meldrum P. 2017. 4D geophysical monitoring of landslide processes: The Hollin Hill case study. *Geophysics 82: B41-B57.*

Watlet A, Van Camp M, Francis O, Poulain A, Hallet V, Triantafyllou A, Delforge D. 2018. Time-lapse electric resistivity tomography to portray infiltration and hydrologic flow paths from surface to cave. *Journal of Hydrology 566: 737-751.*

Whiteley JS, Chambers JE, Uhlemann S, Wilkinson PB, Kendall JM. 2019. Geophysical monitoring of moisture-induced landslides: A review. *Reviews of Geophysics 57: 106-145.*

Zhao Y, Hu Z, Liu Y, Zhang X. 2020. Field experiment on the spatiotemporal evolution of soil moisture in a rainfall-induced loess landslide: Implications for early warning. *Journal of Hydrology 591: 125603.*